Technical Report

UDC 536 . 45 : 681 . 3

Image Measurement of High Temperature Objects

Yusuke KONNO* Yoshito ISEI
Masato SUGIURA

Abstract

Image measurement is suitable for high-temperature objects moving at high speed in steel-making processes because it enables non-contact measurement. The image measurement of the heated objects is classified into two types. One is passive measurement which takes a thermal image. The other is active measurement in which thermal radiation behaves as disturbance light. As example cases of these measurement technologies, a quantification method for a combustion field inside a blast furnace raceway, multiple sensing of a molten iron stream tapped from a blast furnace, and strip position detection and shape measurement implemented in a hot rolling process are described in this paper.

1. Introduction

At an integrated steel plant, first, iron ore is reduced at more than 2000°C in a blast furnace and it turns to molten pig iron of 1500°C. In the next steelmaking process, the molten iron is charged into a converter and oxygen is supplied to refine it. The temperature of the molten iron increases from 1500°C to 1700°C quickly. The refined molten steel is solidified in a continuous caster to produce steel slabs. In the hot rolling process, a steel slab 200 to 300 mm thick heated to 1200°C is rolled into a thin steel strip a few mm thick with hot-rolling mills. The speed of the steel strip that is discharged from the last mill stand is 25 m/s at maximum. The strip is rapidly cooled at high speed to form appropriate microstructure. In these dynamic manufacturing processes, measurement is a very important elemental technology. In the steel industry, the facilities used are large and the temperatures of materials processed are extremely high. Such measurement conditions are unique to the steel industry.

This paper focuses on the measurement of high-temperature objects in the steel production processes and describes the following image measurement methods that Nippon Steel & Sumitomo Metal Corporation has researched and developed for internal manufacturing processes as examples: 1) Quantification of conditions of combustion fields inside blast furnace raceways at 2000°C,[1)] 2) multiple measurement of various factors (e.g., temperature and flow rate) of fluid that is a mixture of molten iron and slag discharged from blast furnaces at 1500°C,[2–4)] and 3) position detection and shape measurement of strips on hot rolling lines at 1000°C.[5, 6)]

2. Optical Measurement of Red-hot Objects

This section consolidates approaches to measure objects accompanying thermal radiation optically while referring to the blackbody radiation theory. According to Planck's law of blackbody radiation, an object emits thermal radiation depending on its temperature. **Figure 1** shows blackbody spectral radiance as a function of wavelength at various temperatures. When an object is heated to approximately 700°C, red light becomes clearly recognizable to the human eye. In this temperature range, the dominant spectrum of radiance is

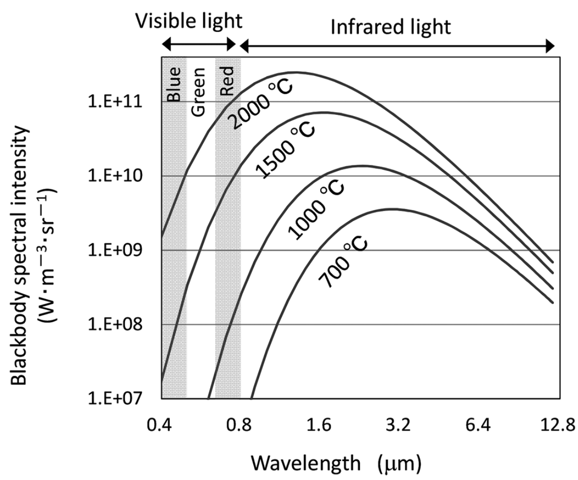

Fig. 1 Spectral intensity of blackbody radiation

* Chief Researcher, Instrumentation & Control Research Lab., Process Research Laboratories
20-1 Shintomi, Futtsu City, Chiba Pref. 293-8511

infrared rays. As the temperature increases, the radiance increases and the wavelength of the spectrum peak shifts to the short wavelength side. At 1 000°C, the radiance of visible light is ten times or more that at 700°C, so in active image measurement with light projection, thermal radiation behaves as disturbance. Therefore, the type of light source to be used and wavelength to be measured by a camera need to be appropriately determined. Around 1 000°C, the thermal radiation in the visible range is mostly red, so an optical filter is attached to a camera to shut off red to near infrared spectrums and a blue lighting is used in general image measurement.

Thermal radiation works as disturbance for light to be measured. In addition to such problem, in the steel industry where a large quantity of materials is processed in high-temperature processes, the temperature around the equipment used and exposed to heat radiation also becomes high. Therefore, thermal protection of measuring instruments to be installed in the manufacturing fields is also important. When it is 1 500°C or higher, the thermal radiation in the visible range is so intense that the options for lighting with luminance that can overcome such light intensity are very small. For a red-hot object, a CCD camera or CMOS camera with spectral sensitivity in the visible range can be used to take thermal images. Compared to another type of thermal image observation in which an infrared camera is used to take images from normal to medium temperatures, a visible light camera can easily control imaging such as high-speed exposure and high frame rate and its resolution is also high. Therefore, to obtain data on the luminance distribution on hot objects (luminance differences depending on temperature), passive image measurement using visible light cameras is useful.

3. Thermal Image Measurement Targeting Blast Furnaces

A blast furnace is the symbol of an integrated steel plant. Sintered iron ore and coke (carbonized coal) are charged from the blast furnace top. Hot blasts are blown in from the tuyeres in the lower section of the body and burned to reduce iron oxides contained in the iron ore to produce molten iron. A large blast furnace with the inner capacity of more than 5 000 m^3 produces 10 000 tons or more molten iron per day. The molten iron is then supplied to processes for manufacturing various types of products, such as sheets, plates, section steel, and steel tubes and pipes, via the steelmaking process. The temperature and pressure inside a blast furnace is high. At the lower section of a blast furnace at which the temperature exceeds the melting point of iron, in particular, putting probes into the furnace is very difficult. Understanding the conditions inside blast furnaces that cannot be directly measured in detail is a constant requirement to operate them stably. Nippon Steel & Sumitomo Metal has been working to create measurement technologies to understand the conditions from tuyeres to hearths in the lower sections of blast furnaces for which only limited measurement data could be obtained.

3.1 Technology to quantify the combustion fields in blast furnace tuyeres

At the end of a blast furnace tuyere, there is a hollow cavity called a raceway that was formed by the entry of hot blasts. To improve the reactivity, pulverized coal (PC) is blown in from a PC lance in the tuyere. These conditions affect the stability of blast furnace operation, so blast furnace tuyeres have inspection holes, from which operators visually check and judge the conditions inside the furnace based on their experience. Recently, various steelmakers have introduced a system in which a camera is installed into each tuyere to monitor the conditions of the furnace from the control room remotely in place of visual checks.[1, 7] A blast furnace has approximately 40 tuyeres, so if images from such cameras are visually observed, it is difficult to record and quantify temporal changes and spatial changes in the circumference direction of the furnace. Therefore, Nippon Steel & Sumitomo Metal started developing an image processing method to extract characteristics from the camera image containing two-dimensional spatial and one-dimensional temporal data from tuyere cameras.[1] This technology makes it easier to compare obtained data to past operation data and search similar cases.

3.1.1 Tuyere images and their characteristic conditions

Figure 2 shows typical tuyere camera image patterns. Figure 2a) shows the normal state where the flow of the pulverized coal jetted out from a PC lance is stable and the radiation from the high temperature field at 2 000°C in the furnace is uniform. Figure 2b) shows that the flow of the pulverized coal is unstable and the flow direction changes both in terms of time and space. This is possibly because the shape of the raceway changed, which may have disturbed the gas flow. In Fig. 2c), many pieces of dark unmolten ore and coke flow down from the top of the image—dark means their temperatures are low. This state indicates that the formed raceway is unstable.

3.1.2 Procedures for obtaining feature values

When the size of an image is W pixels in width and H pixels in length, it is handled as vector data in $W \times H$ dimensions in signal processing. As general methods for dimensionality reduction of high-dimensional data (e.g., image data), principal component analysis, independent component analysis, and sparse modeling are often used. However, we adopted staged reduction focusing on the characteristics of the tuyere images. **Figure 3** shows the entire flow.

First, the contour at the end of a tuyere nozzle was ellipse-fitted. The contour of the nozzle in tuyere camera image $I(x, y, t)$ is constantly moving because the temperature field is not uniform due to hot blasts. Therefore, the contour in each frame needs to be tracked to capture the luminance of the periphery accurately. Ellipse parameters of the center and major and minor axes that were calculated by elliptic approximation of the contour in each frame are used to obtain normalized images $I_n(x, y, t)$ through affine conversion such that they have a nominal center and nominal radius.

The position of the PC lance varies from tuyere to tuyere and abnormal combustion spreads from the center toward the outside, so only a component of the radial direction was extracted and compressed. Specifically, normalized image I_n was turned into $I_p(r, \theta, t)$ through polar conversion. I_p was binarized to calculate the projection in the θ direction ($P(r, t) = \Sigma_\theta I_{bin}(r, \theta, t)$) in binary image $I_{bin}(r, \theta, t)$.

Figure 4 shows projection $P(r, t)$ corresponding to the states in Fig. 2. Temporal changes cannot be overlooked in original moving

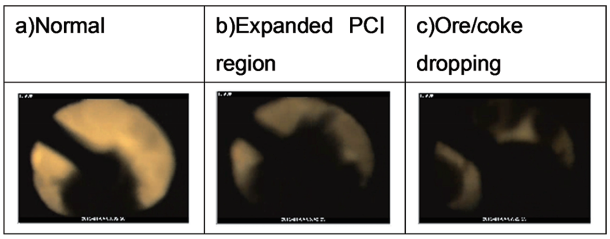

PCI: Pulverized coal injection

Fig. 2 Examples of tuyere images

image $I(x, y, t)$. However, compressing the data to a two-dimensional map enables observation of temporal changes. Under the normal state in Fig. 4a), the state in the radial and time directions remains uniform. Figure 4b) (abnormal combustion at the PC) shows that the luminance at the center decreases once and then recovers gradually. Figure 4c) in which ore drops shows that the entire image turns dark.

As feature values to distinguish the three states extracted from $P(r, t)$, average $H_1(t)$ for r of $P(r, t)$ and its peak location $H_2(t)$ were finally adopted.

$$H_1(t) = \frac{1}{b-a} \sum_{r=a}^{b} P(r,t) \tag{1}$$

$$H_2(t) = \arg\max_{r} P(r,t) \tag{2}$$

3.1.3 Comparison of proposed feature values and tuyere camera images

Figure 5 shows feature values $H_1(t)$ and $H_2(t)$ calculated from $P(r, t)$ shown in Fig. 4. Under the normal state in Fig. 5a), both feature values are high, but in abnormal combustion at the PC in Fig. 5b), only $H_1(t)$ significantly decreases. In Fig. 5c) where ore drops, both $H_1(t)$ and $H_2(t)$ significantly decrease. **Figure 6** shows these three states plotted on a plane of H_1-H_2. This figure shows that the normal domain, abnormal combustion at the PC, and dropping of ore are located in different domains from each other.

As described above, dimensionality reduction focusing on the characteristics of the tuyere camera images allowed the moving images of high-dimensional data to be compressed to only two-dimensional data. Using a distance on a feature plane as the scale makes it easier to compare data to past operation data and search a history. We will examine, in addition to temporal changes for a single tuyere, the distribution of proposed features for tuyeres in the peripheral direction of a furnace to reveal the relationship between

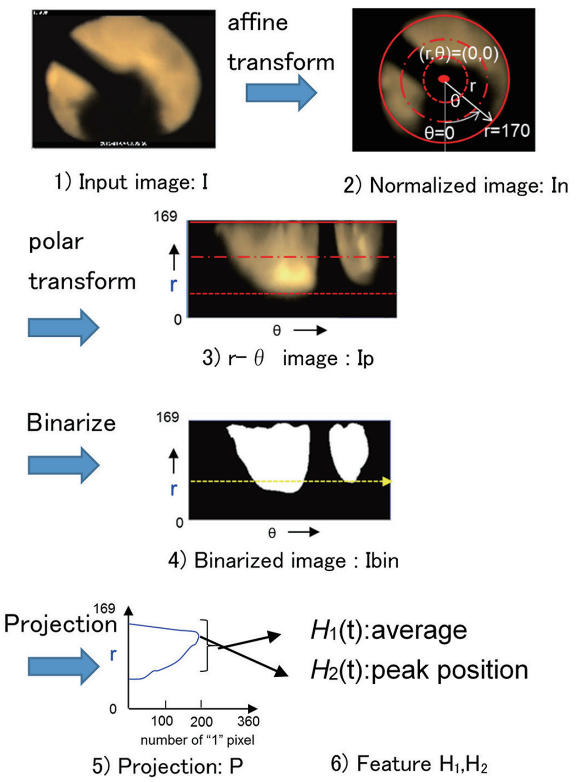

Fig. 3 Feature extraction diagram

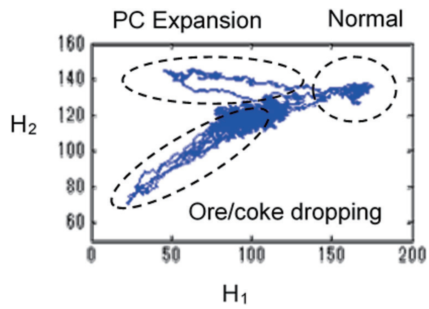

Fig. 6 Plotting of feature values H_1-H_2 plane

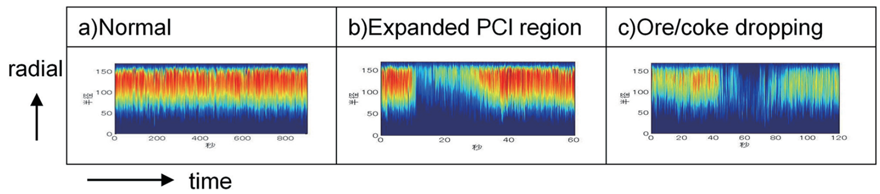

Fig. 4 Time series of projection $P(r,t)$

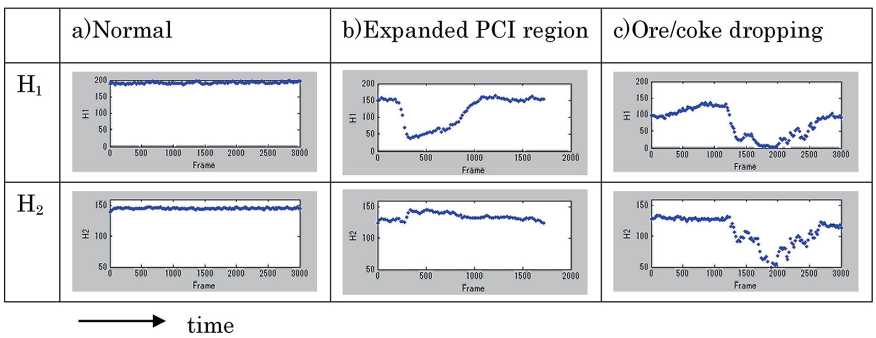

Fig. 5 Time series of extracted feature values $H_1(t)$, $H_2(t)$

them and macroscopic conditions of a blast furnace.

3.2 Monitoring of blast furnace tapping stream

Molten iron and slag (by-product) drip and build up pool at the hearth of a blast furnace. Slag is a mixture of oxides (e.g., CaO, Al_2O_3, SiO_2, and MgO) contained in iron ore. When a hole is bored on a refractory wall with a drill, molten iron containing slag flows out. This high-temperature fluid is called a tapping stream. Usually, tapping takes approximately three hours each time. Multiple tap holes are opened one by one to discharge molten iron. The tapping stream possibly shows the condition of the high temperature field of the hearth that cannot be directly observed. We have developed an image measurement technology to calculate the temperature of the tapping stream, ratio of slag contained, and exit velocity from thermal images.

3.2.1 Thermal images of tapping stream

Figure 7 is a thermal image of the tapping stream from when it is discharged from a tap hole to when it reaches the trough taken at a high-speed exposure to avoid blurs. The tapping stream is 1 400°C to 1 600°C, glowing at a high intensity. On the tapping stream, molten iron is separated from slag in a mottled way. The rather dark domains are molten iron and brighter domains are slag. The tapping stream is a turbulent flow where the mottled patterns of slag change during the flow moment by moment.

The temperatures of molten iron and slag in the same furnace are similar, but their emissivity is different, so their radiances vary. **Figure 8** is an optical model of the tapping stream's thermal radiation. Molten iron is opaque since it is a metal. Its radiance (L_M) is a function of the surface temperature and emissivity. Therefore,

$$L_M = \varepsilon_M L_b(T) \tag{3}$$

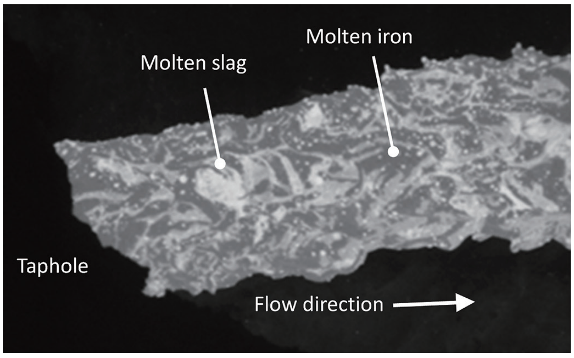

Fig. 7 Example of thermal image of molten iron stream

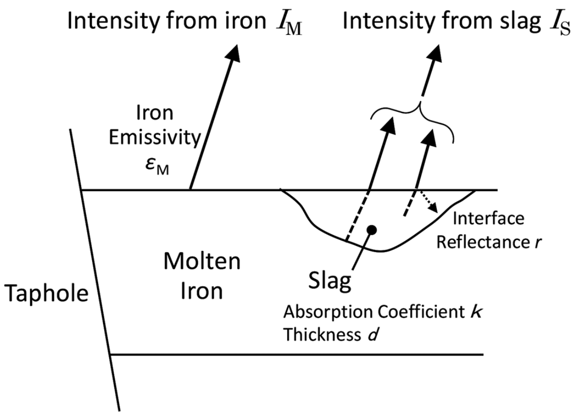

Fig. 8 Thermal radiation model of molten slag/iron

Where, $L_b(T)$ is the blackbody radiance at temperature T and ε_M is the molten iron's emissivity.

Figure 7 shows the intensity in the molten iron domains is almost uniform, but the intensity of the slag varies spot by spot. This is because slag is optically semitransparent and thereby the emissivity varies depending on its thickness. The slag's radiance (L_S) is expressed with the Formula (4).[2] The first term on the right side of the Formula (4) is a component of the molten iron radiance passed through the slag. The second term is the radiance of the slag itself. Both radiances are the function of the thickness of slag (d). The Formula (5) organizes the radiances of the molten iron and slag.

$$L_S = (1-r)e^{-kd}\cdot\varepsilon_M + (1-r)\cdot(1-e^{-kd})\cdot L_b(T) \tag{4}$$

$$= (1-r)\cdot(e^{-kd}\cdot\varepsilon_M + 1 - e^{-kd})\cdot L_b(T) \tag{5}$$

Where, r is the reflectivity at the interface between the slag and the atmosphere.

3.2.2 Measurement of the temperatures of molten iron and slag

The temperatures of molten iron and slag are measured by determining the representative intensity through turning images into a histogram and by a radiation thermometry technique. **Figure 9** shows an example histogram of the intensity in a thermal image of the tapping stream. The histogram shape changes depending on the temperature and the ratio of slag. The intensity distribution of molten iron always has a clear peak (P in the figure), so this value is used as the representative intensity of the molten iron to calculate its temperature while referring to the predetermined calibration data of image intensity and temperature. Repeating these image processing procedures enables continuous thermometry.

However, the slag's radiance changes depending on its thickness, so the intensity distribution on the histogram is broad without a clear peak and thereby the method for the molten iron cannot be applied to it. Therefore, we focused on the maximum intensity (M in the figure) on the thermal image. The maximum intensity (M) is observed in a rather large slag pattern, where the slag layer may be thick and the emissivity may be stable at a high level. When slag is thick and molten—iron radiation cannot go through it, its emissivity is 0.9 or higher when calculated from the optical constants of slag.

3.2.3 Measurement of the ratio of slag, exit velocity, and tapping stream diameters

As shown with the broken lines in Fig. 9, the intensity distribution of molten iron always partly overlaps with that of slag. Therefore, simple image binarization cannot separate them. To separate the intensity distribution of molten iron from that of slag on a histo-

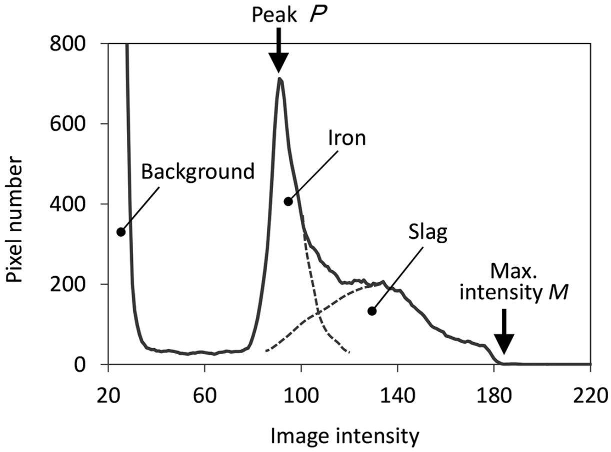

Fig. 9 Histogram of thermal image

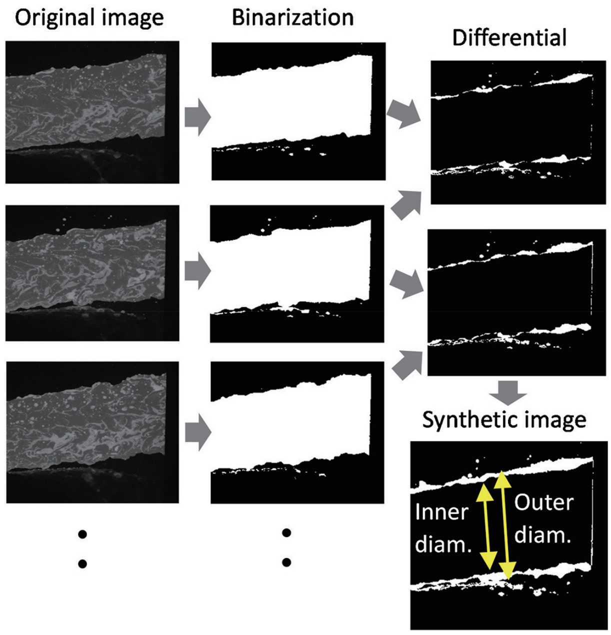

Fig. 10 Image processing of diameter measurement

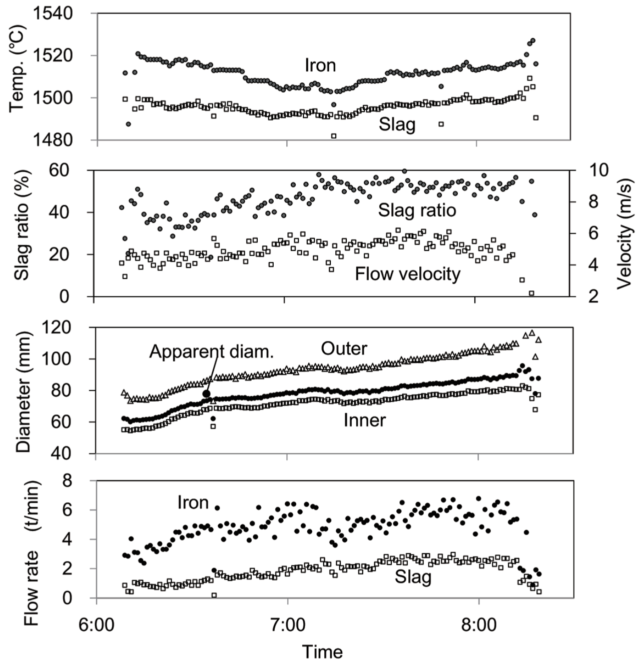

Fig. 11 Examples of field experiment data

gram, for example, Gaussian function is fitted to the distribution of the molten iron and slag and the area ratio of their Gaussian distribution is used as the ratio between the molten iron and slag.[3)]

Tapping stream is a turbulent flow moving at approximately 5 m/s. Photographing the flow of molten iron and slag at 200 frames per second makes enables observation that their patterns are gradually changing. The tapping stream speed can be calculated by taking successive images like this and following the travel distance of the tapping stream images with correlation calculation.[4)]

The tapping stream involves always transforming surface waves. As shown in **Fig. 10**, first, tapping stream images are extracted through binarization from multiple thermal images photographed in a short time; second, only sections where the waveform was changed are extracted through differential processing of two successive binarized images; and then such images are overlapped to make a composite image. The narrowest part of the domain with the waves on the composite image is determined as the inner diameter and the largest part is determined as the outer diameter. The apparent tapping stream diameter required to calculate the tapping amount is located between the inner and outer diameters, so the location is experimentally determined so as to match the weighed value of the molten iron. From the ratio of slag, velocity, and apparent tapping stream diameter measured, the flow rate of the molten iron and slag can be continuously learned.

3.2.4 Field experiment results

Figure 11 shows the observation results of one tapping. In commercial operation, the temperature of molten iron is measured with a disposable thermocouple only once an hour and the total amount of tapped molten iron is weighed. Our image measurement technique can measure the temperature of molten iron and slag and the flow rate of tapped molten iron continuously. Our experiments have revealed irregular temperature fluctuation, differences in the temperatures between molten iron and slag, unevenness of the slag ratios between tap holes, and other conditions that used to be unknown. This is probably because the hearths in blast furnaces are in an unsteady state and the phenomena are expected to be clarified.

4. Image Measurement of Hot Rolling of Sheets

The hot rolling processes for manufacturing hot-rolled steel sheets have heating furnaces, roughing-down mills, finishing mills, cooling zones, and coilers. Steel slabs heated to 1 200°C in a reheating furnace are rolled into rough bars with a roughing mill. A finishing mill consisting of six or seven rolling stands is used to roll the bars to the target thickness. The strips are then cooled and wound with a coiler. In today's hot rolling processes, a strip 200 to 300 mm thick is rolled to 1.2 to a few mm only in a few minutes and they are wound into coils. At this time, the rolling speed is 25 m/s at maximum and accuracy in the thickness is a few tens μm. In the processes for high-temperature steel sheets, high-speed processing and high dimension accuracy have been realized. The temperature during hot rolling is 800°C to 1 000°C and that is lower than that of blast furnaces for making molten iron. However, strips handled in the hot-rolling processes are closer to finished products, so measuring instruments to be used need to be highly accurate and have high responsivity to achieve high dimension accuracy and required microstructure.

The blackbody radiation in Fig. 1 shows that the spectral radiance from the object in the temperature range from 800°C to 1 000 °C is red (0.6 μm) to infrared. CCD and CMOS cameras generally used for image measurement detect wavelengths from 0.4 μm to 1.1 μm. Therefore, there are two image measurement methods for hot rolling: One to directly take an image of high-temperature radiation (0.6 μm to 1.1 μm) and the other in which light having a shorter wavelength (0.4 μm to 0.6 μm) than the red is projected to take an image of the reflected light.

Recently, the response and resolution of two-dimensional imaging devices have been improving and the processing speed of computers to be used for image processing has been increasing year by year, allowing expansion of the scope to which image processing can be applied in hot rolling. Using two-dimensional images is good for improving the stability and accuracy of measurement.

4.1 Interstand strip position sensor

Strips need to be stably threaded to secure the productivity in the finishing rolling. The tail end of a thin steel strip being rolled moves sideways abnormally between rolling mill stands due to a slight error in the leveling setting of the mill stands (parallelism of the reduction rollers). The strip may come into contact with the side guides and rolled in folds. This problem called strip pincher damages the work rolls and then they need to be replaced, which decreases the productivity. Therefore, we have developed a technology to measure strip walking at the tail end between stands at high-speed response and control the leveling of rolling mill stands by feeding data back to reduce strip pincher.

Previously, high-resolution and high-responsivity line sensors were used to detect the positions of the edges of strips being hot-rolled to measure their width and positions. However, a line sensor measures one point in the rolling direction, so if the target point is covered with waterdrops, steam, fumes, and other disturbance factors, it cannot detect the edge position. Such disturbance often occurs between finishing mill stands which are very close to each other, and that makes it difficult to measure strip positions stably. Using a two-dimensional camera to image a strip in a wide field of view and measuring the edge position through image processing work well against such problems.

Figure 12 illustrates the configuration of an inter-stand strip position sensor in a two-dimensional camera method installed between finishing mill stands.[5] This strip position sensor takes an image of a high-temperature (red hot) strip using high-speed, two-dimensional cameras at a high frame rate and measures the edge position by image processing to calculate the strip position. In addition, two two-dimensional cameras are used to obtain a stereoscopic vision of a strip, capable of measuring changes in the distance from the cameras to the strip. Part of the strip edge in the field of view may be obstructed due to mists and fumes between finishing stands. To solve such a problem, we have devised a method to detect edges shown in **Fig. 13**. First, a candidate edge on each scan line is detected by searching a position at which the differential intensity is maximum. Next, the regression line for the detected candidate edge positions on all the scan lines calculated by the least squares method is regarded as the strip edge line.

In the least squares method, the differential intensity is used as a weight coefficient to reduce the influence of the scan lines with indistinct edges. This method has made it possible to detect the strip position even when the view is partly obstructed by mists and fumes and to output the measured strip position with a resolution of 1 mm or less 80 times or more per second. When a steel strip has tension, the camber of the strip itself tends to become dominant, so behavior between stands is the same as that on the exit side. **Figure 14** compares values measured by the strip position sensor installed between the last stands and those measured by the existing line sensor on the exit side. After the tip of the strip reaches the down coiler and after tension is applied, the two types of measured values are almost the same. That shows that the strip position sensor works well.

4.2 Strip shape meter at a mill exit

Recently, in hot strip rolling, manufacturing high-tensile steel sheets stably and highly accurately is an important task. In the rolling of high-tensile steel sheets, loads (by rolling) are high, so work rolls bend significantly, which tends to make the elongation in the width direction uneven. When the elongation at the center of the width is larger, the strip has center buckles. When it is larger at the edge(s), the strip has edge waves. These defects in the shape cause problems with threading and non-uniform temperature in the cooling zone. Therefore, we have developed a technology to measure the shape of a strip at the exit of the finishing mill, calculate the elongation distribution in the width direction, and feed the information back to the shape control actuator of the rolling stands.

Conventionally, twin-beam distance meter methods[8, 9] were commonly used to measure the shape of strips at the exit of the rolling mill. In the method, two laser range finders installed in the rolling direction are used to measure the inclination angle of the surface momentarily to calculate the surface length. To control rolling stands, elongation distribution in the width direction needs to be measured. There are two twin-beam methods: One in which multiple measuring heads are arranged in the width direction to measure the elongation distribution and the other in which two parallel laser lines are projected across the width to perform measurements by the laser light-section method. However, in these methods, the measurement accuracy worsens when strip waviness due to shape defects

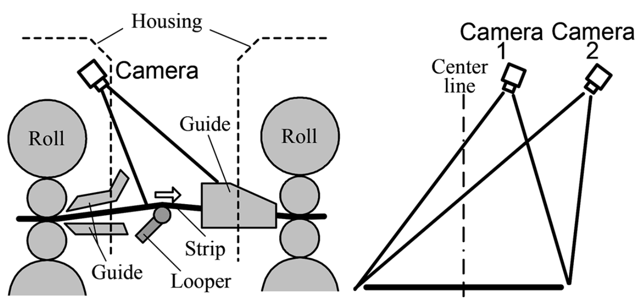

Fig. 12 Layout of inter-stand strip position sensor

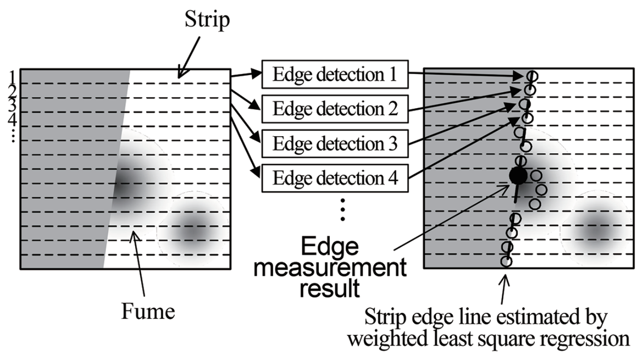

Fig. 13 Edge measurement method

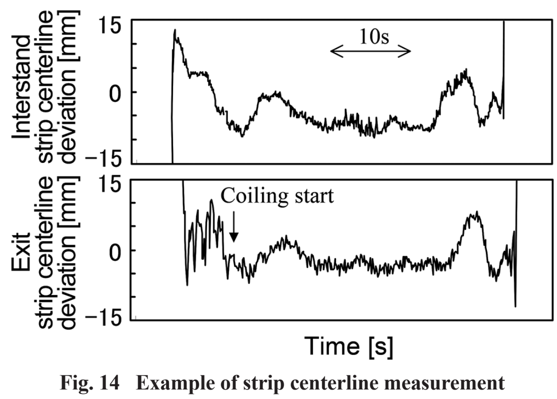

Fig. 14 Example of strip centerline measurement

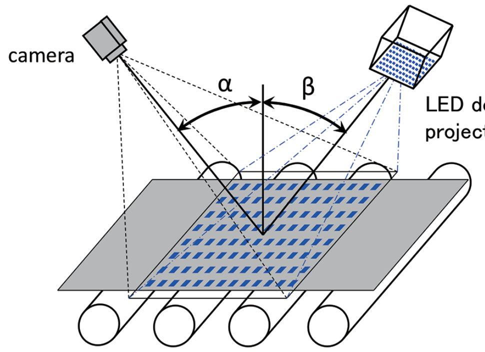

Fig. 15 Configuration of shape meter using LED dot pattern projection method

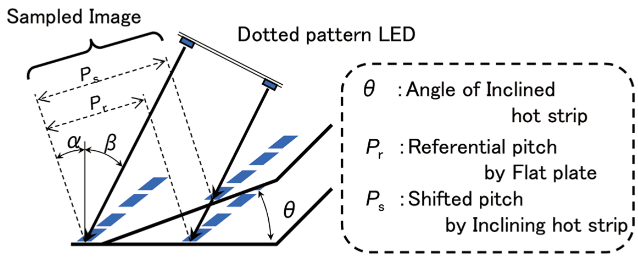

Fig. 16 Principle of shape measurement method

forms a standing wave with a rolling stand as the fixed end and waves observed seem stationary.

Today, for the promotion of energy saving in the lighting sector, the optical power and efficiency of LED light sources are rapidly increasing. Power LED chips for which the emission intensity per 1 W of input exceeds 100 lm have even appeared. Nippon Steel & Sumitomo Metal used such LED chips to develop a shape meter with the LED dot pattern projection method.[6, 10] In this method, power LED chips are arranged two-dimensionally to form a periodic pattern and this pattern is projected onto the surface of a strip. High-luminance blue LED chips and an optical filter that passes only blue light are used to take images, which makes it possible to observe patterns projected on the surface of a hot strip clearly. **Figure 15** illustrates the configuration of the shape meter. **Figure 16** shows the principle of measuring an inclination angle of the surface. The LED projector places a two-dimensional lattice pattern in a wide range onto the surface of a strip and the two-dimensional camera takes images of the projected lattice pattern from a different direction. At this time, the pattern pitch changes depending on the inclination angle of the surface.

When α is the angle of the camera's optical axis, β is the angle of the projector, P_r is the reference pitch of the flat sheet, and P_s is the pitch of the inclination of the steel strip, the inclination angle of the surface (θ) is expressed with the Formula (6).

$$\theta = \tan^{-1}\left(\frac{(P_s/P_r)-1}{\tan\alpha + (P_s/P_r)\tan\beta}\right) \qquad (6)$$

The surface length of a strip and the elongation can be calculated by measuring the pattern pitch distribution in the projected pattern in an image, calculating the angle distribution on the surface of the strip, and line integrity of the angle distribution in the designated section in the rolling direction. **Figure 17** shows example measurement results. The strip shape meter measures the shape within the field of view instantaneously and calculates the elongation. Therefore, it can reduce degradation of the accuracy when standing waves are formed. It also realized stable strip shape measurement (success rate of measurement is 98.5% or higher) and longer service life of light sources because high-luminance LED dot pattern projection is applied.

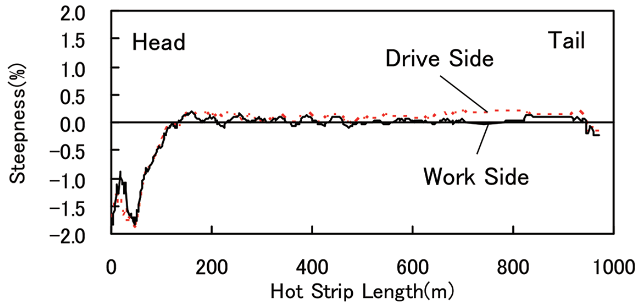

Fig. 17 Example of online steepness measurement

5. Conclusions

This paper introduced image measurement methods in the blast furnace and hot rolling processes. Although the cases introduced are special methods targeting high-temperature objects emitting light, we achieved high-performance field measurement by understanding thermal radiation and devising appropriate imaging methods. As Nippon Steel & Sumitomo Metal has been developing measurement technologies internally, it has been accumulating knowledge and expertise on environmental technologies such as heatproofing and dustproofing sensors to be installed at manufacturing sites. The number of sensors used is smaller when the environment on manufacturing lines is more severe, so expectations for new measurement technologies are high as solutions for process events and input of control loops. As the business environment around steelmaking is becoming harsher, for example, due to global competition and consideration for the global environment, Nippon Steel & Sumitomo Metal will continue researching and developing measurement technologies that will overcome these severe environments unique to the steelmaking processes and that contribute to both production and quality improvement.

References

1) Konno, Y. et al.: CAMP-ISIJ. 27, 326 (2014)
2) Sugiura, M. et al.: Proceedings of SICE Annual Conference 2011. 2011, p.472
3) Sugiura, M. et al.: Int. J. Thermophysics. 35, 1320 (2014)
4) Sugiura, M. et al.: Proceedings of the 57th Japan Joint Automatic Control Conference. 2014, p.367
5) Washikita, Y. et al.: Tetsu-to-Hagané. 95 (1), 43 (2009)
6) Katoh, T. et al.: CAMP-ISIJ. 24, 888 (2011)
7) Yamahira, H. et al.: CAMP-ISIJ. 28, 203 (2015)
8) Yamane, T. et al.: CAMP-ISIJ. 2, 1540 (1989)
9) Toyoda, T. et al.: Tetsu-to-Hagané. 70 (9), 1071 (1984)
10) Ohta, T. et al.: CAMP-ISIJ. 25, 352 (2012)


Yusuke KONNO
Chief Researcher
Instrumentation & Control Research Lab.
Process Research Laboratories
20-1 Shintomi, Futtsu City, Chiba Pref. 293-8511


Masato SUGIURA
Senior Researcher, Ph.D.
Instrumentation & Control Research Lab.
Process Research Laboratories


Yoshito ISEI
Senior Researcher
Instrumentation & Control Research Lab.
Process Research Laboratories